

## Research Article

# Synthesis of Directional Sources Using Wave Field Synthesis, Possibilities, and Limitations

E. Corteel<sup>1,2</sup>

<sup>1</sup> IRCAM, 1 Place Igor Stravinsky, 75004 Paris, France

<sup>2</sup> Sonic Emotion, Eichweg 6, 8154 Oberglatt, Switzerland

Received 28 April 2006; Revised 4 December 2006; Accepted 4 December 2006

Recommended by Ville Pulkki

The synthesis of directional sources using wave field synthesis is described. The proposed formulation relies on an ensemble of elementary directivity functions based on a subset of spherical harmonics. These can be combined to create and manipulate directivity characteristics of the synthesized virtual sources. The WFS formulation introduces artifacts in the synthesized sound field for both ideal and real loudspeakers. These artifacts can be partly compensated for using dedicated equalization techniques. A multichannel equalization technique is shown to provide accurate results thus enabling for the manipulation of directional sources with limited reconstruction artifacts. Applications of directional sources to the control of the direct sound field and the interaction with the listening room are discussed.

Copyright © 2007 E. Corteel. This is an open access article distributed under the Creative Commons Attribution License, which permits unrestricted use, distribution, and reproduction in any medium, provided the original work is properly cited.

## 1. INTRODUCTION

Wave field synthesis (WFS) is a physics-based sound reproduction technique [1–3]. It allows for the synthesis of wave fronts that appear to emanate from a virtual source at a defined position. WFS thus provides the listener with consistent spatial localization cues over an extended listening area.

WFS mostly considers the synthesis of virtual sources exhibiting omnidirectional directivity characteristics. However, the directive properties of sound sources contribute to immersion and presence [4], both notions being related to spatial attributes of sound scenes used in virtual or augmented environments. Directivity creates natural disparities in the direct sound field at various listening positions and governs the interaction with the listening environment.

This article focuses on the synthesis of the direct sound associated to directional sources for WFS. In a first part, an extended WFS formulation is proposed for the synthesis of elementary directional sources based on a subset of spherical harmonics. The latter are a versatile representation of a source field enabling a flexible manipulation of directivity characteristics [4]. We restrict on the derivation of WFS for a linear loudspeaker array situated in the horizontal plane. Alternative loudspeaker geometries could be considered following a similar framework but are out of the scope of this article. This array can be regarded as an acoustical aperture

through which an incoming sound field propagates into the listening area. Therefore, directivity characteristics of virtual sources may be synthesized and controlled only in a single plane through the array only, generally the horizontal plane.

The generalized WFS formulation relies on approximations that introduce reproduction artifacts. These artifacts may be further emphasized by the nonideal radiation characteristics of the loudspeakers. Equalization techniques are thus proposed for the compensation of these artifacts in a second part. A third part compares the performance of the equalization schemes for the synthesis of elementary directional sources and composite directivity characteristics. A last part discusses applications of directional sources for the manipulation of the direct sound in an extended listening area and the control of the interaction of the loudspeaker array with the listening environment.

## 2. SYNTHESIS OF DIRECTIONAL SOURCES USING WFS

The common formulation of WFS relies on two assumptions [2, 3, 5, 6]:

- (1) sources and listeners are located within the same horizontal plane;
- (2) target sound field emanates from point sources having omnidirectional directivity characteristics.

The first assumption enables one to derive a feasible implementation based on linear loudspeaker arrays in the horizontal plane. Using the second assumption, the sound field radiated by the virtual source can be extrapolated to any position in space. Loudspeaker (secondary source) input signals are then derived from an ensemble of approximations of the Rayleigh 1 integral considering omnidirectional secondary sources [2, 3, 5, 6].

An extension of WFS for the synthesis of directional sources has been proposed by Verheijen [7]. The formulation considers general radiation of directive sources assuming *far field* conditions. In this section, we propose an alternative definition of WFS filters for directional sources that considers a limited ensemble of spherical harmonics. This versatile and flexible description allows for comprehensive manipulation of directivity functions [4]. It also enables us to highlight the various approximations necessary to derive the extended WFS formulation and the artifacts they may introduce in the synthesized sound field. This includes near field effects that are not fully described in Verheijen's approach [7].

### 2.1. Virtual source radiation

Assuming independence of variables (radius  $r$ , elevation  $\delta$ , azimuth  $\phi$ ), spherical harmonics appear as elementary solutions of the wave equation in spherical coordinates [8]. Therefore, the radiation of any sound source can be decomposed into spherical harmonics components.

Spherical harmonics  $Y_{mn}(\phi, \delta)$  of degree  $m$  and of order  $0 \leq n \leq |m|$  are expressed as

$$Y_{mn}(\phi, \delta) = P_n^m(\cos \delta) \Phi_m(\phi), \quad (1)$$

where

$$\Phi_m(\phi) = \begin{cases} \cos(m\phi) & \text{if } m \geq 0, \\ \sin(|m|\phi) & \text{if } m < 0, \end{cases} \quad (2)$$

and  $P_n^m$  are Legendre polynomials.

$Y_{mn}(\phi, \delta)$  therefore accounts for the angular dependency of the spherical harmonics. The associated radial term ( $r$  depending solution of the wave equation) is described by divergent  $h_n^-$  and convergent  $h_n^+$  spherical Hankel functions.

Considering the radiation of a source in free space, it is assumed that the sound field is only divergent. The radiation of any sound source is therefore expressed as a weighted sum of the elementary functions  $\{h_n^- Y_{mn}, 0 \leq n \leq |m|, m, n \in \mathbb{N}\}$ :

$$P(\phi, \delta, r, k) = \sum_{m=-\infty}^{+\infty} \sum_{0 \leq n \leq |m|} B_{mn}(k) h_n^-(kr) Y_{mn}(\phi, \delta), \quad (3)$$

where  $k$  is the wave number and coefficients  $B_{mn}$  are the modal strengths.

### 2.2. Derivation of WFS filters

WFS targets the synthesis in a reproduction subspace  $\Omega_R$  of the pressure caused by a virtual source  $\Psi_{mn}$  located in a

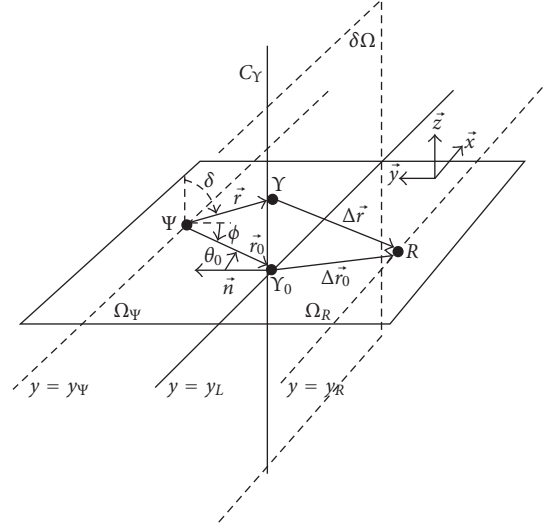


FIGURE 1: Synthesis of the sound field emitted by  $\Psi$  using the Rayleigh 1 integral.

“source” subspace  $\Omega_\Psi$  (see Figure 1).  $\Psi_{mn}$  has radiation characteristics of a spherical harmonic of degree  $m$  and order  $n$ .  $\Omega_R$  and  $\Omega_\Psi$  are complementary subspaces of the 3D space. According to Rayleigh integrals framework (see, e.g., [9]), they are separated by an infinite plane  $\partial\Omega$ . Rayleigh 1 integral states that the pressure caused by  $\Psi_{mn}$  at position  $r_R \in \Omega_R$  is synthesized by a continuous distribution of ideal omnidirectional secondary sources  $Y$  located on  $\partial\Omega$  such that

$$p(r_R) = -2 \int_{\partial\Omega} \frac{e^{-jk\Delta r}}{4\pi\Delta r} \vec{\nabla} (h_n^-(kr) Y_{mn}(\phi, \delta)) \cdot \vec{n} dS, \quad (4)$$

where  $\Delta r$  denotes the distance between a given secondary source  $Y$  and  $r_R$ . The angles  $\delta$  and  $\phi$  are defined as the azimuth and elevation in reference to the virtual source position  $r_\Psi$  (see Figure 1).

The gradient of the spherical harmonic is expressed as

$$\begin{aligned} & \vec{\nabla} (h_n^-(kr) Y_{mn}(\phi, \delta)) \\ &= \frac{\partial h_n^-(kr)}{\partial r} Y_{mn}(\phi, \delta) \vec{e}_r \\ &+ \left( \frac{1}{r} \frac{\partial Y_{mn}}{\partial \delta}(\phi, \delta) \vec{e}_\delta + \frac{1}{r \sin \delta} \frac{\partial Y_{mn}}{\partial \phi}(\phi, \delta) \vec{e}_\phi \right) h_n^-(kr). \end{aligned} \quad (5)$$

In (4), the considered virtual source input signal is a Dirac pulse. Therefore, the derived secondary source input signals are impulse responses of what is referred to as “WFS filters” in the following of the article.

#### 2.2.1. Restriction to the horizontal plane

Using linear loudspeaker arrays in the horizontal plane, only the azimuthal dependency of the source radiation can be synthesized. The synthesized sound field outside of the horizontal plane is a combination of the radiation in the horizontal

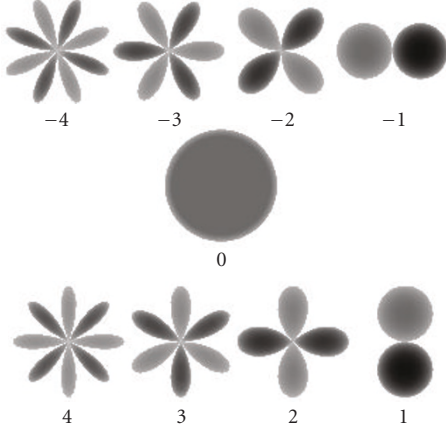


FIGURE 2: Elementary directivity functions, sources of degree  $-4$  to  $4$ .

plane and the loudspeakers' radiation characteristics. Considering the synthesis of spherical harmonics of degree  $m$  and order  $n$ , the order  $n$  is thus simply undetermined. It should be chosen such that the  $P_n^m(0) \neq 0$  ( $\delta = \pi/2$ ). This condition is fulfilled for  $n = |m|$  since

$$P_n^m(x) = (-1)^m (2m-1)! (1-x^2)^{m/2}. \quad (6)$$

In the following, we consider that  $n = |m|$  and refer to a virtual source  $\Psi_m$  of degree  $m$ . The radiation characteristics of a subset of such elementary directivity functions, sources of degree  $m$ , are described in Figure 2.

### 2.2.2. Simplification of the pressure gradient

Using far field assumption ( $kr \gg 1$ ),  $h_n^-(kr)$  is simplified as [10]

$$h_n^-(kr) \simeq \frac{j^{n+1} e^{-jkr}}{kr}. \quad (7)$$

Similarly, the  $r$  derivative term of (5) becomes

$$\frac{dh_n^-(kr)}{dr} Y_{mn}(\phi, \delta) \simeq -jk \frac{j^{n+1} e^{-jkr}}{kr} Y_{mn}(\phi, \delta). \quad (8)$$

In the following, the term  $j^{n+1}$  is omitted for simplification of the expressions.

In the horizontal plane ( $\delta = \pi/2$ ), the  $\phi$  derivative term of (5) is expressed as

$$\frac{1}{r} \frac{\partial \widetilde{Y}_{mn}}{\partial \phi} \left( \phi, \frac{\pi}{2} \right) = \frac{P_n^m(0)}{r} \times \begin{cases} -m \sin(m\phi) & \text{if } m \geq 0, \\ m \cos(m\phi) & \text{if } m < 0, \end{cases} \quad (9)$$

where  $\times$  denotes the multiplication operator. This term may vanish in the far field because of the  $1/r$  factor. However, we will note that the zeros of  $Y_{mn}(\phi, \pi/2)$  in the  $r$  derivative term of (5) correspond to nonzero values of the  $\phi$  derivative term

(derivative of cos function is the sin function and vice versa). Therefore, in the close field and possibly large  $|m|$  values, the  $\phi$  derivative term may become significant in (5).

The  $\delta$  derivative term of (5) is not considered here since it simply vanishes in the loudspeaker geometry simplification illustrated in the next section.

### 2.2.3. Simplification of the loudspeaker geometry

The WFS formulation is finally obtained by substituting the secondary source distribution along column  $C_Y(x)$  (cf. Figure 1) with a single secondary source  $Y_0(x)$  at the intersection of column  $C_Y(x)$  and the horizontal plane. This requires compensation factors that modify the associated driving functions. They are derived using the so-called stationary phase approximation [2].

In the following, bold letters account for the discrete time Fourier transform (DTFT) of corresponding impulse responses. The WFS filter  $\mathbf{u}_{\Psi_m}(x, \omega)$  associated to a secondary source  $Y_0(x)$  for the synthesis of a virtual source  $\Psi_m$  is derived from (4) as

$$\mathbf{u}_{\Psi_m}(x, k) = \sqrt{\frac{k}{2\pi}} g_{\Psi} \cos \theta_0 \frac{e^{-j(kr_0 - \pi/4)}}{\sqrt{r_0}} \Phi_m(\phi), \quad (10)$$

considering low values of absolute degree  $|m|$  and assuming that the source is in the far field of the loudspeaker array ( $kr \gg 1$ ). In this expression,  $\omega$  denotes the angular frequency and  $\omega = k/c$  where  $c$  is the speed of sound. The 0 subscript corresponds to the value of the corresponding parameter in the horizontal plane.  $\theta_0$  is defined such that  $\cos \theta_0 = \mathbf{e}_r \cdot \mathbf{n}$ . Note that the  $\delta$  derivative term of (5) vanishes since  $\mathbf{e}_\delta \cdot \mathbf{n} = 0$  in the horizontal plane. The  $\phi$  derivative term of (5) is removed for simplicity, assuming far field conditions and small  $|m|$  values. However, we will see that this may introduce artifacts in the synthesized sound field.

$g_{\Psi}$  is a factor that compensates for the level inaccuracies due to the simplified geometry of the loudspeaker array:

$$g_{\Psi} = \sqrt{\frac{|y_{R_{\text{ref}}} - y_L|}{|y_{R_{\text{ref}}} - y_{\Psi}|}}. \quad (11)$$

The compensation is only effective at a reference listening distance  $y_{R_{\text{ref}}}$ . Outside of this line, the level of the sound field at position  $r_R$  can be estimated using the stationary phase approximation along the  $x$  dimension [11]. The corresponding attenuation law  $Att_{\Psi_m}$  is expressed as

$$Att_{\Psi_m}(r_R) = \sqrt{\frac{|y_{R_{\text{ref}}}|}{|y_R|}} \sqrt{\frac{|y_R| + |y_{\Psi_m}|}{|y_{R_{\text{ref}}}| + |y_{\Psi_m}|}} \frac{1}{4\pi d_{\Psi_m}^R}, \quad (12)$$

assuming  $y_L = 0$  for simplicity.  $d_{\Psi_m}^R$  denotes the distance between the primary source  $\Psi_m$  and the listening position

$r_R$ . It appears as a combination of the natural attenuation of the target virtual source ( $1/4\pi d_{\Psi_m}^R$ ) and of the line array ( $\sqrt{1/|y_R|}$ ).

The proposed WFS filters  $\mathbf{u}_{\Psi_m}(x, \omega)$  are consistent with the expression proposed by Verheijen [7] where his frequency dependent  $G(\phi, 0, \omega)$  factor is substituted by the frequency independent  $\Phi_m(\phi)$  factor. The proposed expression appears thus as a particular case of Verheijen's formulation. However, the frequency dependency may be reintroduced by using frequency dependent weighting factors of the different elementary directivity functions  $\Phi_m$  as shown in (3). As already noticed, the spherical harmonic based formulation however highlights the numerous approximations necessary to derive the WFS filters without a priori far field approximation.

The WFS filters are simply expressed as loudspeaker position and virtual source dependent gains and delays and a general  $\sqrt{k}e^{j(\pi/4)}$  filter. In particular, delays account for the "shaping" of the wave front that is emitted by the loudspeaker array.

### 2.3. Limitations in practical situations

In the previous part, the formulation of the WFS filters is defined for an *infinitely long continuous* linear distribution of *ideal* secondary sources. However, in practical situations, a *finite* number of *regularly spaced real* loudspeakers are used.

#### 2.3.1. Rendering artifacts

Artifacts appear, such as

- (i) diffraction through the finite length aperture which can be reduced by applying an amplitude taper [2, 3],
- (ii) spatial aliasing due to the finite number of loudspeakers [2, 3, 11],
- (iii) near field effects for sources located in the vicinity of the loudspeaker array for which the far field approximations used for the derivation of WFS filters (cf. (10)) are not valid [11],
- (iv) degraded wave front forming since real loudspeakers are not ideal omnidirectional point sources.

Among these points, spatial aliasing limits the sound field reconstruction of the loudspeaker array above a so-called spatial aliasing frequency  $f_{\Psi}^{\text{al}}$ . Contributions of individual loudspeaker do not fuse into a unique wave front as they do at low frequencies [3]. Considering finite length loudspeaker arrays, the aliasing frequency depends not only on the loudspeaker spacing and the source location but also on the listening position [11, 12]. It can be estimated as

$$f_{\Psi}^{\text{al}}(r_R) = \frac{1}{\max_{i=1 \dots I} |\Delta\tau_R^{\Psi}(i)|}, \quad (13)$$

where  $|\Delta\tau_R^{\Psi}(i)|$  is the difference between the arrival time of the contribution of loudspeaker  $i$  and loudspeaker  $i + 1$  at listening position  $r_R$ . The latter can be calculated from the WFS delays of (10) and natural propagation time between loudspeaker  $i$  and listening position  $r_R$ .

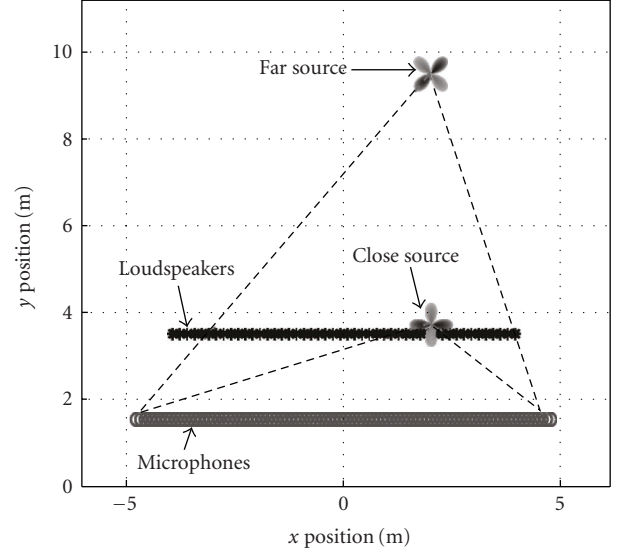


FIGURE 3: Test configuration, 48-channel loudspeaker array, 96 microphones at 2 m, 1 source 20 cm behind the array, 1 source 6 m behind the array.

#### 2.3.2. Simulations

These artifacts are illustrated with the test situation shown in Figure 3. An 8 m long, 48-channel, loudspeaker array is used for the synthesis of two virtual sources:

- (1) a source of degree  $-2$ , located at (2, 6), 6 m behind and off-centered 2 m to the right (far source),
- (2) a source of degree 2, located at (2, 0.2), 20 cm behind and off-centered 2 m to the right (close source).

In order to characterize the emitted sound field, the response of the loudspeaker array is simulated on a set of 96 omnidirectional microphones positioned on a line at 2 m away from the loudspeakers with 10 cm spacing. Loudspeakers are ideal point sources having omnidirectional characteristics. The response is calculated using WFS filters (see (10)) and applying the amplitude taper to limit diffraction [2].

Figure 3 further displays the portion of the directivity characteristics of both sources that is synthesized on the microphones (dashed lines). It can be seen that a smaller portion of the directivity characteristics of the far source, compared to the close source, is synthesized on the microphones. In the case of the far source, the right line also shows visibility limitations of the source through the extent of the loudspeaker array. For the far source, the few microphones located at  $x > 4.5$  m are not anymore in the visibility area of the source.

Figures 4(a) and 5(a) display frequency responses  $\mathbf{w}_{\Psi_m}(r_j, \omega)$  of the loudspeaker array for the synthesis of both the far and close sources of Figure 3 on all microphone positions  $r_j$ ,  $j = 1 \dots 96$ . Figures 4(b) and 5(b) show the frequency responses of a quality function  $q_{\Psi_m}$  that describes the deviation

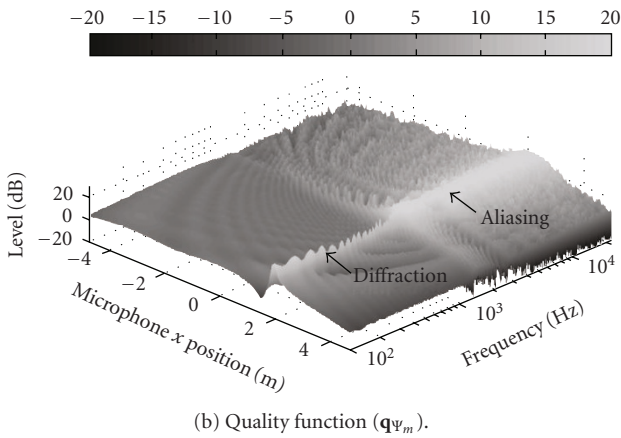
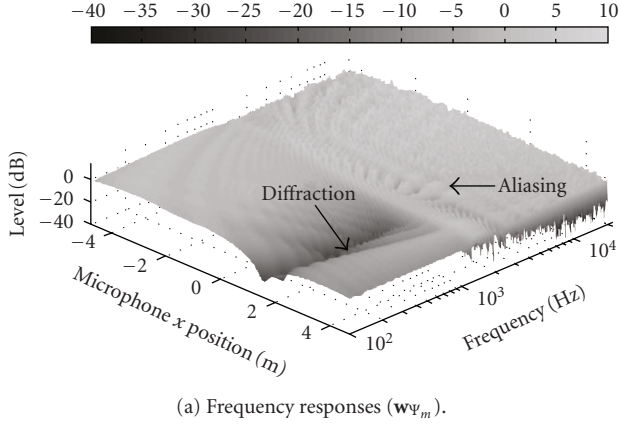


FIGURE 4: Frequency responses ( $\mathbf{w}_{\Psi_m}$ ) and quality function ( $\mathbf{q}_{\Psi_m}$ ) of an 8 m, 48-channel, loudspeaker array simulated on a line at 2 m from the loudspeaker array for synthesis of a source of degree  $-2$  (far source of Figure 3).

of the synthesized sound field from the target. It is defined as

$$\mathbf{q}_{\Psi_m}(r_j, \omega) = \frac{\mathbf{w}_{\Psi_m}(r_j, \omega)}{\mathbf{a}_{\Psi_m}(r_j, \omega)}, \quad (14)$$

where  $\mathbf{a}_{\Psi_m}(r_j, \omega)$  is the “ideal” free-field WFS frequency response of an infinite linear secondary source distribution at  $r_j$ :

$$\mathbf{a}_{\Psi_m}(r_j, \omega) = Att_{\Psi_m}(r_j) \Phi_m(\phi(r_j, r_{\Psi})) e^{-jk(|r_j - r_{\Psi}|)}. \quad (15)$$

$Att_{\Psi_m}(r_j)$  is the attenuation of the sound field synthesized by an infinite linear secondary source distribution (see (12)).  $\Phi_m(\phi(r_j, r_{\Psi}))$  corresponds to the target directivity of the source  $\Psi_m$  at  $r_j$ .

For both close and far sources, the target directivity characteristics are not reproduced above a certain frequency which corresponds to the spatial aliasing frequency (see Figures 4 and 5). This is a fundamental limitation for the spatially correct synthesis of virtual sources using WFS.

Diffraction artifacts are observed in Figure 4 for the synthesis of the far source. They remain observable despite the

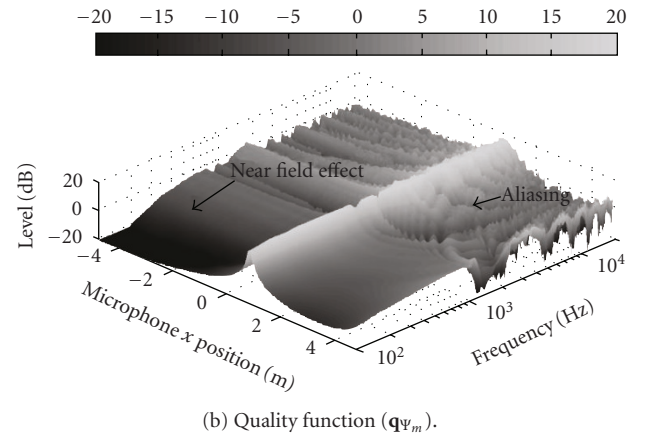
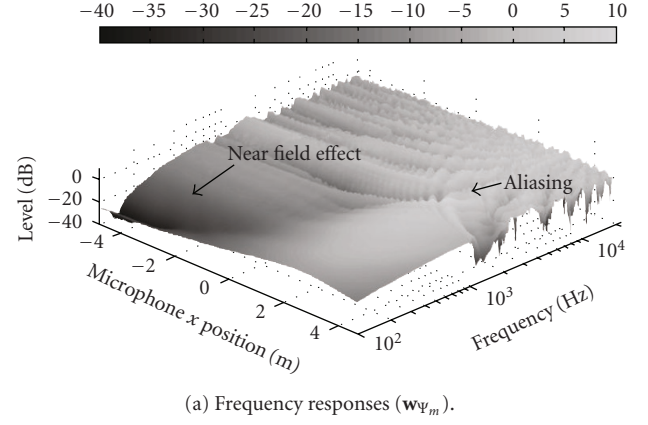


FIGURE 5: Frequency responses ( $\mathbf{w}_{\Psi_m}$ ) and quality function ( $\mathbf{q}_{\Psi_m}$ ) of an 8 m, 48-channel, loudspeaker array simulated on a line at 2 m from the loudspeaker array for synthesis of a source of degree  $+2$  (close source of Figure 3).

amplitude tapering [11]. They introduce small oscillations at mid and low frequencies and limit the proper synthesis of the null of the directivity characteristics for microphone positions around  $x = 2$  m.

For the close source being situated at 20 cm from the loudspeaker array, the far field approximations used for the derivation of the WFS filters of (10) are not valid anymore. Near-field effects can thus be observed (see Figure 5). The directivity characteristics of this source imposes the synthesis of two nulls at  $x = 0$  and  $x = 4$  m which are not properly reproduced. Moreover, the frequency responses at microphone positions in the range  $x \in [-4, \dots, -2]$  m exhibit high-pass behavior. More generally, the synthesis of such sources combines several factors that introduce synthesis inaccuracies and limit control possibilities:

- (1) the visibility angle of the source through the loudspeaker array spans almost  $180^\circ$ , that is, a large portion of the directivity characteristics have to be synthesized which is not the case for sources far from the loudspeaker array;

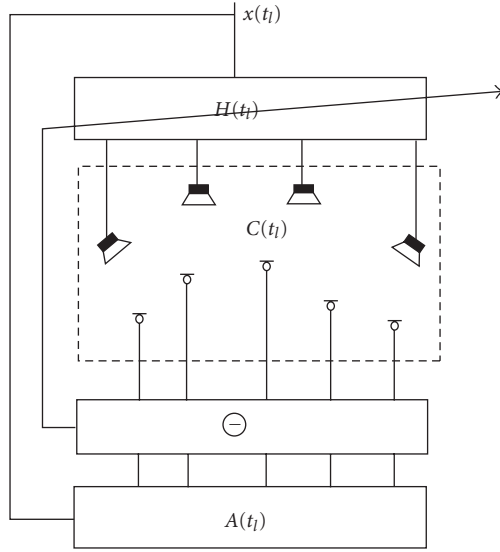


FIGURE 6: Equalization for sound reproduction.

- (2) only few loudspeakers have significant level in the WFS filters (cf. (10)) and may contribute to the synthesis of the sound field.

### 3. EQUALIZATION TECHNIQUES FOR WAVE FIELD SYNTHESIS

It was shown in the previous section that the synthesis of elementary directivity function using WFS exhibits reproduction artifacts even when ideal loudspeakers are used. In this section, equalization techniques are proposed. They target the compensation of both real loudspeaker's radiation characteristics and WFS reproduction artifacts.

Equalization has originally been employed to compensate for frequency response impairments of a loudspeaker at a given listening position. However, in the context of multichannel sound reproduction, a plurality of loudspeakers contribute to the synthesized sound field. Listeners may be located within an extended area where rendering artifacts should be compensated for.

In this section, three equalization techniques are presented:

- (i) individual equalization (Ind),
- (ii) individual equalization with average synthesis error compensation (AvCo),
- (iii) multichannel equalization (Meq).

The first two methods enable one to compensate for the spatial average deficiencies of the loudspeakers and/or WFS related impairments. The third method targets the control of the synthesized sound field within an extended listening area.

#### 3.1. Framework and notations

Equalization for sound reproduction is a filter design problem which is illustrated in Figure 6.  $x(t_i)$  denotes the discrete

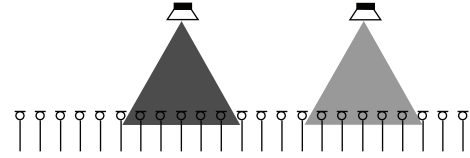


FIGURE 7: Measurement selection for individual equalization.

time (at  $t_i$  instants) representation of the input signal. The loudspeakers' radiation is described by an ensemble of impulse responses  $c_i^j(t_i)$  (impulse response of loudspeaker  $i$  measured by microphone  $j$ ). They form the matrix of signal transmission channels  $C(t_i)$ . The matrix  $C(t_i)$  therefore defines a multi-input multi-output (MIMO) system with  $I$  inputs (the number of loudspeakers) and  $J$  outputs (the number of microphones).

Equalization filters  $h_i(t_i)$ , forming the matrix  $H(t_i)$ , are thus designed such that the error between the synthesized sound field, represented by the convolution of signal transmission channels  $C(t_i)$  and filters  $H(t_i)$ , and a target, described in  $A(t_i)$ , is minimized according to a suitable distance function.

We restrict to the description of the free field radiation of loudspeakers. The compensation of listening room related artifacts is out of the scope of this article. It is considered in the case of WFS rendering in [11, 13–16]

#### 3.2. Individual equalization

Individual equalization (Ind) refers to a simple equalization technique that targets only the compensation of the spatial average frequency response of *each* loudspeaker. Associated filters  $h_i(t_i)$  are calculated in the frequency domain as

$$\mathbf{h}_i(\omega) = J \times \sum_{j=1}^J \frac{|\vec{r}_i - \vec{r}^j|}{\mathbf{c}_i^j(\omega)}, \quad (16)$$

where  $\vec{r}_i$  and  $\vec{r}^j$  represent the positions of loudspeaker  $i$  and microphone  $j$ . The individual equalization filter is thus defined as the inverse of the spatial average response of the corresponding loudspeaker. The upper term of (16) therefore compensates for levels differences due to propagation loss.

Prior to the spatial average computation, the frequency responses  $\mathbf{c}_i^j(\omega)$  may be smoothed. The current implementation employs a nonlinear method similar to the one presented in [16]. This method preserves peaks and compensates for dips. The latter are known to be problematic in equalization tasks.

The current implementation of individual equalization uses only measuring  $j$  positions within a 60 degree plane angle around the main axis of the loudspeaker  $i$  (cf. Figure 7). Filters  $h_i^{\text{ind}}(t_i)$  are designed as 800 taps long minimum phase FIR filters at 48 kHz sampling rate.

### 3.3. Individual equalization with average synthesis error compensation

Individual equalization for wave field synthesis compensates only for the “average” loudspeaker related impairments independently of the synthesized virtual source. However, WFS introduces impairments in the reproduced sound field even using ideal omnidirectional loudspeakers (see Section 2.3). The “AvCo” (average compensation) method described here relies on modified individual equalization filters. It targets the compensation of the spatial average of the synthesis error, described by the quality function  $q_{\Psi_m}^{\text{Ind}}$  of (14), while reproducing the virtual source  $\Psi_m$  using WFS filters of (10) and individual equalization filters  $h_i^{\text{Ind}}(t_l)$ . First,  $q_{\Psi_m}^{\text{Ind}}$  should be estimated for an ensemble of measuring positions  $j$ :

$$\mathbf{q}_{\Psi_m}^{\text{Ind}}(r_j, \omega) = \frac{\sum_{i=1}^J \mathbf{c}_i^j(\omega) \times \mathbf{h}_i^{\text{Ind}}(\omega) \times \mathbf{u}_{\Psi_m}(x_i, \omega)}{\mathbf{a}_{\Psi_m}(r_j, \omega)}. \quad (17)$$

Then, the modified individualization filters  $\mathbf{h}_{i, \Psi_m}^{\text{AvCo}}(\omega)$  are computed in the frequency domain as

$$\mathbf{h}_{i, \Psi_m}^{\text{AvCo}}(\omega) = \frac{J \times \mathbf{h}_i^{\text{Ind}}(\omega)}{\sum_{j=1}^J \mathbf{q}_{\Psi_m}^{\text{Ind}}(r_j, \omega)}. \quad (18)$$

The  $\mathbf{q}_{\Psi_m}^{\text{Ind}}(r_j, \omega)$ 's may also be smoothed prior to the spatial average computation and inversion. Finally, filters  $h_{i, \Psi_m}^{\text{AvCo}}(t_l)$  are designed as 800 taps long minimum phase FIR filters at 48 kHz sampling rate.

Contrary to individual equalization, we will note that the “AvCo” equalization filters  $h_{i, \Psi_m}^{\text{AvCo}}(t_l)$  depend on the virtual source  $\Psi_m$ . However, the error compensation factor (lower term of (18)) does not depend on the loudspeaker number  $i$ . This equalization method may compensate for the spatial average reproduction artifacts for each reproduced virtual source. However, it may not account for position dependent reproduction artifacts. These can be noticed for example in Figure 5(b) for the synthesis of the close source even when ideal omnidirectional loudspeakers are used.

### 3.4. Multichannel equalization

Multichannel equalization [17] consists in describing the multichannel sound reproduction system as a multi-input multi-output (MIMO) system. Filters are designed so as to minimize the error between the synthesized sound field and a target (see Figure 6). The calculation relies on a multichannel inversion process that is realized in the time or the frequency domain.

Multichannel equalization, as such, controls the emitted sound field only at a finite number of points (position of the microphones). However, for wave field synthesis the synthesized sound field should remain consistent within an extended listening area.

A WFS specific multichannel equalization technique has been proposed in [16] and refined in [11, 18]. It targets the compensation of the free field radiation of the loudspeaker system. It combines a description of the loudspeaker array

radiation that remains valid within an extended listening area together with a modified multichannel equalization scheme that accounts for specificities of WFS [18]. The multichannel equalization technique is only briefly presented here. For a more complete description, the reader is referred to [18] or [11].

It is similar to the multichannel equalization techniques recently proposed by Spors et al. [5, 14], López et al. [15], and Gauthier and Berry [6] that target the compensation of the listening room acoustics for WFS reproduction. Note that the proposed technique was also extended to this case [11, 13, 19] but this is out of the scope of this article.

#### 3.4.1. MIMO system identification

The MIMO system is identified by measuring free field impulse responses of each loudspeaker using a set of microphones within the listening area. These are stored and arranged in a matrix  $C(t_l)$  that describes the MIMO system.

The alternative techniques for multichannel equalization in the context of WFS reproduction [5, 14–16] consider a 1-dimensional circular microphone array [5, 14], a planar circular array [15], or a limited number of sensors distributed near a reference listening position in the horizontal plane [6]. They describe the sound field within a limited area that depends on the extent of the microphone array. These solutions consider the problem of room compensation for which the multiple reflections may emanate from any direction. Since only linear loudspeaker arrays are used, the compensation remains limited and suffers from both description and reproduction artifacts [11, 20].

The method considered in this article relies on a regularly spaced linear microphone array at the height of the loudspeakers. It can be shown that this microphone arrangement provides a description of the *main* contributions to the free field radiation of the loudspeakers in the entire horizontal plane [11]. Note that this particular microphone arrangement is also particularly adapted for linear loudspeaker arrays as considered in this article.

#### 3.4.2. Design of desired outputs

The target sound field for the synthesis of source  $\Psi_m$  is defined as the “ideal response” of the loudspeaker array for the synthesis of source  $\Psi_m$ . The target impulse response is defined similar to (15):

$$A_{\Psi_m}(r_j, t) = Att_{\Psi_m}(r_j) \Phi_m(\phi(r_j, r_{\Psi})) \times \delta\left(t - \frac{|r_{\Psi} - r_j|}{c} - \tau_{eq}\right), \quad (19)$$

where  $\tau_{eq}$  is an additional delay in order to ensure that the calculated filters are causal. In the following,  $\tau_{eq}$  is referred to as equalization delay and is set to 150 taps at 48 kHz sampling rate. This particular value provides a tradeoff between equalization efficiency and limitation of preringing artifacts in the filters [18].

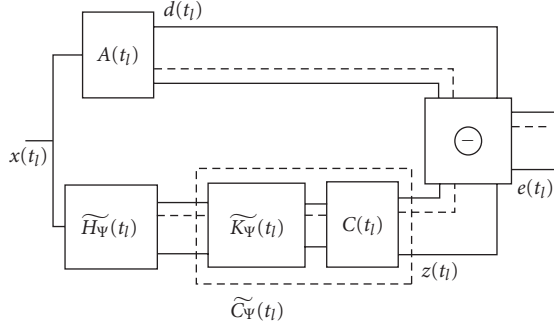


FIGURE 8: Block diagram of the modified inverse filtering process.

### 3.4.3. Multichannel inversion

Filters that minimize the mean square error may be simply calculated in the frequency domain as

$$\mathbf{H}_{0,\text{reg}} = (\mathbf{C}^{*T}\mathbf{C} + \gamma\mathbf{B}^{*T}\mathbf{B})^{-1}\mathbf{C}^{*T}\mathbf{A}, \quad (20)$$

where angular frequency  $\omega$  dependencies are omitted.  $\mathbf{C}^{*T}$  denotes the transposed and conjugate of matrix  $\mathbf{C}$ .  $\mathbf{B}$  is a regularization matrix and  $\gamma$  a regularization gain that may be introduced to avoid ill-conditioning problems [21].

The filters  $\mathbf{H}_{0,\text{reg}}$  account for both wave front forming and compensation of reproduction artifacts. The frequency-based inversion process does not allow one to choose the calculated filters' length. It may also introduce pre-echos, post-echos [22], and blocking effects [23] due to the underlying circular convolution. The latter are due to the circularity of Fourier transform and introduce artifacts in the calculated filters.

A general modified multichannel inversion scheme is illustrated in Figure 8 [11, 18]. We introduce a modified matrix of impulse responses  $\widetilde{\mathbf{C}}_{\Psi_m}(t)$ :

$$\widetilde{c}_{i,\Psi_m}^j(t) = k_{i,\Psi_m}(t) * c_i^j(t), \quad (21)$$

where  $*$  denotes the continuous time domain convolution operator and  $k_{i,\Psi_m}(t)$  is a filter that modifies the driving signals of loudspeaker  $i$  for the synthesis of source  $\Psi_m$  according to a given reproduction technique, for example, WFS. This framework is similar to the one presented by López et al. [15]. However, in our implementation, the filters  $k_{i,\Psi_m}$  only include the delays of WFS filters of (10). WFS gains are omitted since they were found to degrade the conditioning of the matrix  $\widetilde{\mathbf{C}}_{\Psi_m}$  [18].

Filters  $H_{\Psi_m}$  therefore only account for the compensation of reproduction artifacts and not for the wave front forming. This modified multichannel equalization scheme is particularly interesting for WFS since the maximum delay difference considering a ten-meter long loudspeaker array may exceed 1000 taps at 48 kHz sampling rate. This, combined with a multichannel inversion in the time domain, enables one to choose the filter length independently of the length of impulse responses in  $\widetilde{\mathbf{C}}_{\Psi_m}$  and of the virtual source  $\Psi_m$ .

In the following, calculated filters using multichannel equalization are 800 taps long at 48 kHz. They are preferably calculated using an iterative multichannel inverse filtering algorithm derived from adaptive filtering (LMS, RLS, FAP, etc.). The current implementation uses a multichannel version of an MFAP algorithm [11] which provides a good tradeoff between convergence speed and calculation accuracy [24].

### 3.4.4. Above the spatial aliasing frequency

Above the WFS spatial aliasing frequency, multichannel equalization does not provide an effective control of the emitted sound field in an extended area [11]. The proposed multichannel equalization method is therefore limited to frequencies below the spatial aliasing frequency. Down-sampling of  $\widetilde{\mathbf{C}}_{\Psi_m}(t)$  is used to improve calculation speed of the filters. Above the spatial aliasing frequency, the filters are designed using the *AvCo* method presented in the previous section [18].

### 3.4.5. Equalization performances

Figures 9(a) and 9(b) display the frequency responses of the quality function  $\mathbf{q}_{\Psi_m}$  for the synthesis of the two test sources displayed in Figure 3 using filters derived from the multichannel equalization method. These figures should then be compared to, respectively, Figures 4(b) and 5(b). The quality function is almost unchanged above the aliasing frequency. However, diffraction and near-field artifacts are greatly reduced below the aliasing frequency. Remaining artifacts appear mostly at the positions of the nulls of the directional function.

## 4. REPRODUCTION ACCURACY EVALUATION

In this section, the performance of the equalization techniques are compared for both ideal and real loudspeakers. The reproduction accuracy is estimated for a number of virtual sources and listening positions using simple objective criteria.

### 4.1. Test setup

A 48-channel linear loudspeaker array is used as a test rendering setup. The array is 8 m long which corresponds to a loudspeaker spacing of approximately 16.5 cm. Two different types of loudspeakers are considered:

- (i) ideal omnidirectional loudspeakers,
- (ii) multi-actuator panel (MAP) loudspeakers (see Figure 10).

MAP loudspeakers have been recently proposed [16, 25, 26] as an alternative to electrodynamic "cone" loudspeakers for WFS. The large white surface of the panel vibrates through the action of several electrodynamic actuators. Each actuator works independently from the others such that one panel is equivalent to 8 full-band loudspeakers. Tens to hundreds of loudspeakers can be easily concealed in an existing

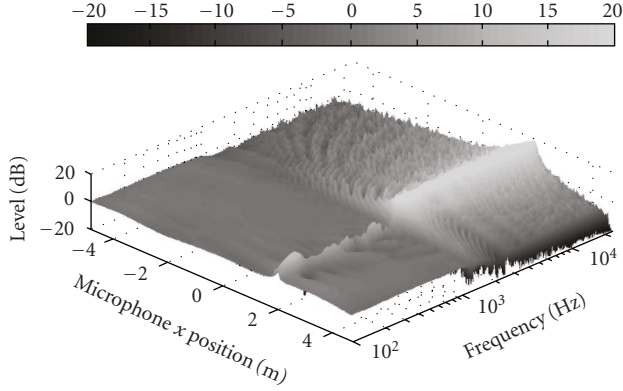
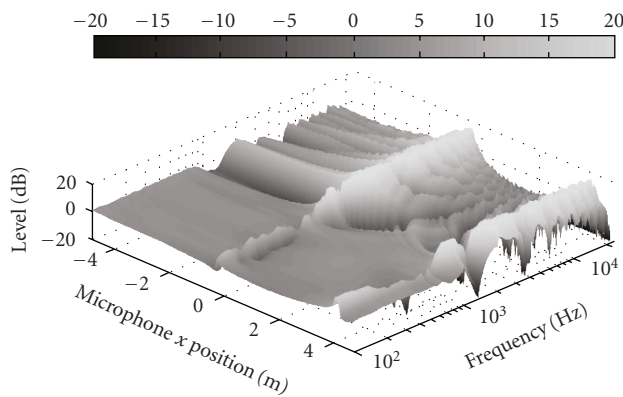
(a) Quality function ( $q_{\Psi_m}$ ) for far source of Figure 3.(b) Quality function ( $q_{\Psi_m}$ ) for close source of Figure 3.

FIGURE 9: Frequency responses ( $w_{\Psi_m}$ ) and quality function ( $q_{\Psi_m}$ ) of an 8 m, 48-channel, loudspeaker array simulated on a line at 2 m from the loudspeaker array for synthesis of the two sources displayed in Figure 3. Filters are calculated using the multichannel equalization method.



FIGURE 10: MAP loudspeakers.

environment given their low visual profile. However, they exhibit complex directivity characteristics that have to be compensated for [11, 16].

The radiation of the 48-channel MAP array has been measured in a large room. The loudspeakers were placed far enough (at least 3 m) from any reflecting surface so it was possible to extract their free field radiation only. The microphones were positioned at four different distances to the loudspeaker array ( $y = -1.5$  m,  $-2$  m,  $-3$  m,  $-4.5$  m, see

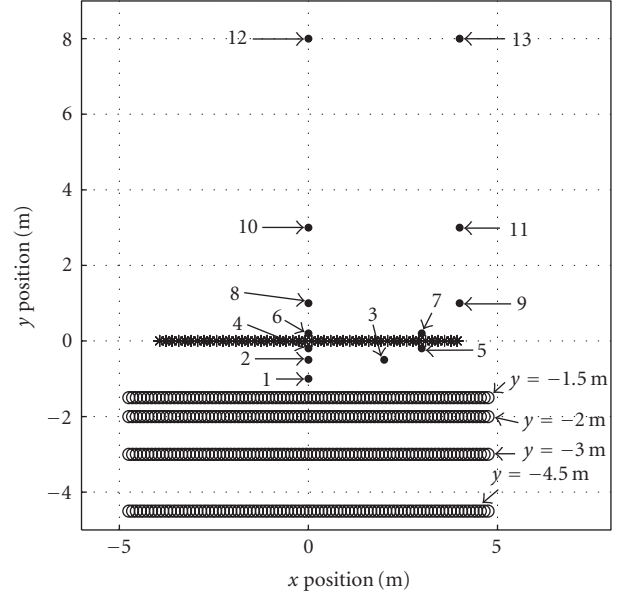


FIGURE 11: Top view of the considered system: 48 regularly spaced (16.75 cm) loudspeakers (\*) measured on 4 depths ( $y = -1.5$ ,  $-2$ ,  $-3$ ,  $-4.5$  m) with 96 regularly spaced (10 cm) microphones (circle) reproducing 13 test sources (dot).

Figure 11). On each line, impulse responses were measured at 96 regularly spaced (10 cm) omnidirectional microphone positions. For ideal loudspeakers, impulse responses of each loudspeaker were estimated on virtual omnidirectional microphones at the same positions.

Equalization filters are designed according to the 3 methods. The 96 microphones situated at  $y = -2$  m (at 2 m from the loudspeaker array) are used to describe the MIMO system. Therefore, the reproduction error should be minimized along that line. However, equalization should remain effective for all other positions. A test ensemble of 13 virtual sources (see Figure 11) is made of

- (i) 5 “focused” sources located at 1 m (centered), 50 cm, and 20 cm (centered and off centered) in front of the loudspeaker array (sources 1/2/3/4/5),
- (ii) 8 sources (centered and off centered) behind the loudspeaker array at 20 cm, 1 m, 3 m, and 8 m (sources 6/7/8/9/10/11/12).

The chosen test ensemble represents typical WFS sources reproduced by such a loudspeaker array. It spans possible locations of virtual sources whose visibility area cover most of the listening space defined by the microphone arrays. In the proposed ensemble, some locations correspond to limit cases for WFS (focused sources, sources close to the loudspeaker array, sources at the limits of the visibility area).

#### 4.2. Reproduction accuracy criteria

The reproduction accuracy may be defined as the deviation of the synthesized sound field compared to the target. It can

be expressed in terms of magnitude and time/phase response deviation compared to a target. Both may introduce perceptual artifacts such as coloration or improper localization. They may also limit reconstruction possibilities of directivity functions as a combination of elementary directivity functions.

At a given listening position  $r_j$ , the magnitude and the temporal response deviation are defined as the magnitude and the group delay extracted from the quality function  $q_{\Psi_m}(r_j, \omega)$  of (14).

The frequency sensitivity of the auditory system is accounted for by deriving the magnitude  $MAG_{\Psi_m}(r_j, b)$  and the group delay deviations  $GD_{\Psi_m}(r_j, b)$  in an ensemble of auditory frequency bands  $ERB_N(b)$  [27]. They are calculated as average values of the corresponding quantities for frequencies  $f = \omega/2\pi$  lying in  $[ERB_N(b - 0.5) \cdot \cdot \cdot ERB_N(b + 0.5)]$  where  $c$  is the speed of sound.

96  $ERB_N$  bands are considered covering the entire audible frequency range. The evaluation is however limited for frequency bands between 100 Hz and the aliasing frequency above which the directivity characteristics cannot be synthesized. Small loudspeakers have to be used for WFS because of the relatively small spacing between the loudspeakers (typically 10–20 cm). Therefore, the lower frequency of 100 Hz corresponds to their typical cut-off frequency. For the considered loudspeaker array, virtual source positions, and listening positions, the aliasing frequency is typically between 1000 and 2000 Hz according to (13). 30 to 40  $ERB_N$  bands are thus used for the accuracy evaluation depending both on the source and the listening position.

In the following, the reproduction accuracy is estimated for a large number of test parameters (frequency band, listening positions, source position and degree, equalization method). Therefore, more simple criteria should be defined. The mean value and the standard deviation of  $MAG_{\Psi_m}(r_j, b)$  or  $GD_{\Psi_m}(r_j, b)$  calculated for an ensemble of test parameters are proposed as such criteria.

The mean value provides an estimate of the overall observed deviation. Such a global deviation may typically be a level modification (for  $MAG_{\Psi_m}$ ) or a time shift (for  $GD_{\Psi_m}$ ) which is possibly not perceived as an artifact. However, a nonzero mean deviation for a given elementary directivity function may introduce inaccuracies if combined with others.

The standard deviation accounts for the variations of the observed deviation within the ensemble of test parameters. It can thus be seen as a better indicator of the reproduction accuracy.

### 4.3. Results

The aim of this section is to compare the performances of the three equalization methods described in Section 3 for both ideal and MAP loudspeakers. Reproduction accuracy is estimated first for the synthesis of elementary directivity functions (see Figure 2).

Spherical harmonic framework enables one to synthesize composite directivity functions as a weighted sum of

elementary directivity functions. This reduces the dimensionality of the directivity description but suppose that each elementary function is perfectly synthesized or, at least, with limited artifacts. Therefore, accuracy of composite directivity functions is considered in Sections 4.3.2 and 4.3.3.

#### 4.3.1. Synthesis of elementary directivity functions

Equalization filters have been calculated for all sources of the test setup (cf. Figure 11) considering elementary directivity functions of degree  $-4$  to  $4$ . For each source position, each elementary directivity function and each equalization method  $MAG_{\Psi_m}$  and  $GD_{\Psi_m}$  are calculated at all microphone positions. The mean value and the standard deviation of  $MAG_{\Psi_m}$  are derived for each equalization method considering three test parameter ensembles:

- (1) all measuring positions, all source degrees, individually for each source position (source position dependency);
- (2) all measuring positions, all source positions, individually for each source degree (source degree dependency);
- (3) all source positions, all source degrees, and all measuring positions, individually for each measuring distance to the loudspeaker array (measuring distance dependency).

Figures 12 and 13 show mean values (mean, lines) and standard deviation (std, markers) of  $MAG_{\Psi_m}$  evaluated below the aliasing frequency for the three test ensembles. They show comparison between individual equalization (Ind), individual equalization + average synthesis error compensation (AvCo) and multichannel equalization (Meq) for both ideal (cf. Figure 12) and MAP (cf. Figure 13) loudspeakers. In the case of ideal loudspeakers, no loudspeaker related impairments have to be compensated for. Therefore, the filters calculated with the individual equalization method are simple WFS filters of (10).

Similar behavior is observed for both ideal and MAP loudspeakers. The standard deviation of  $MAG_{\Psi_m}$  is generally higher for MAP loudspeakers (from 0.2 to 1 dB) than for ideal loudspeakers. This is due to the more complex directivity characteristics of these loudspeakers that can only be partly compensated for using the various equalization methods.

As expected, the *Ind* method provides the poorest results both in terms of the mean value and the standard deviation of  $MAG_{\Psi_m}$ . The *AvCo* method enables one to compensate for the mean values inaccuracies. However, no significant improvements are noticed on standard deviation values. The *Meq* method performs best having mean values remaining between  $-0.5$  and  $0.5$  dB and a standard deviation at least 1 dB lower than other methods for all situations. These are significant differences that may lead to audible changes (reduced coloration, increased precision for manipulation of source directivity characteristics, etc.).

Sources close the loudspeaker array (4/5/6/7) have worst results. This is coherent with the general comments on this

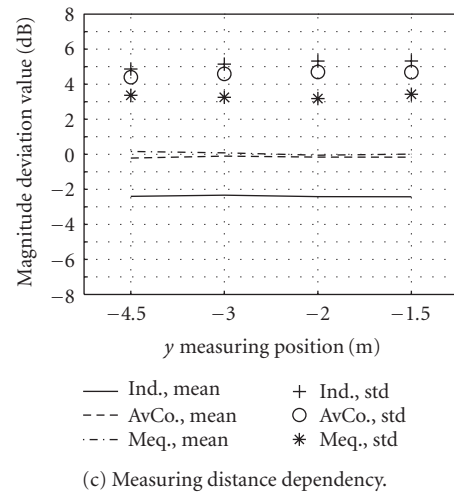
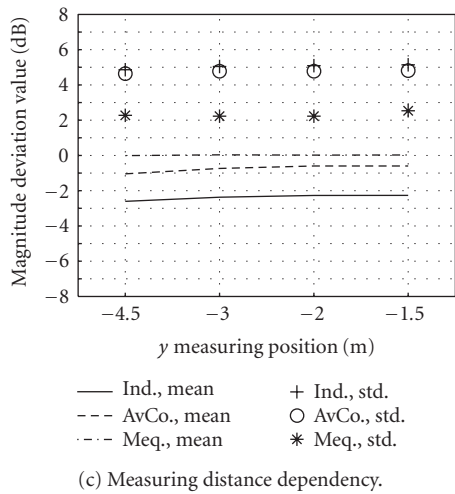
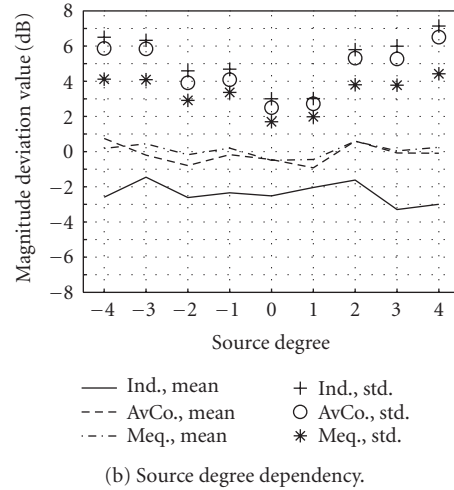
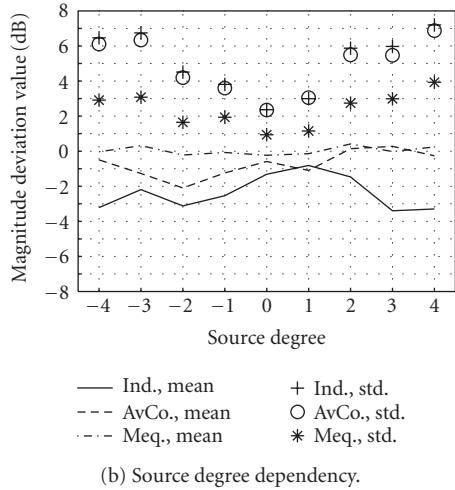
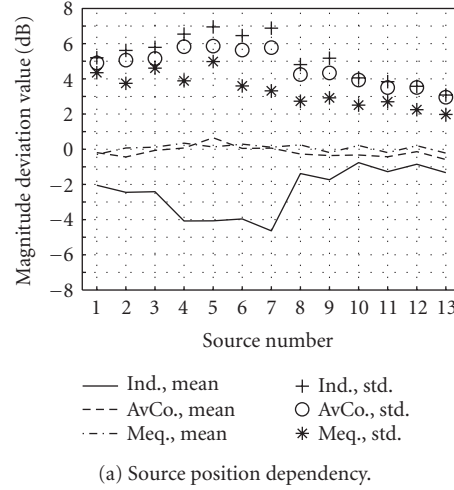
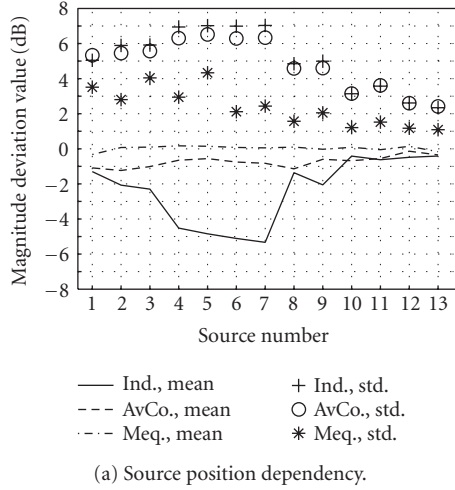


FIGURE 12: Mean value (mean) and standard deviation (std) of  $MAG_{\psi_m}$  evaluated below the aliasing frequency for all microphone and source positions. Comparison between individual equalization (Ind), individual equalization + average synthesis error compensation (AvCo), and multichannel equalization (Meq) for ideal loudspeakers.

FIGURE 13: Mean value (mean) and standard deviation (std) of  $MAG_{\psi_m}$  evaluated below the aliasing frequency for all microphone and source positions. Comparison between individual equalization (Ind), individual equalization + average synthesis error compensation (AvCo), and multichannel equalization (Meq) for MAP loudspeakers.

TABLE 1: Mean value and standard deviation  $GD_{\text{ERB}}$  for all microphone positions, all source positions and degrees.

	Ideal		MAP	
	Mean	Std	Mean	Std
Ind	-0.02 ms	1.27 ms	1.39 ms	1.70 ms
AvCo	0.05 ms	1.27 ms	1.36 ms	1.67 ms
Meq	0.09 ms	1.23 ms	0.90 ms	1.39 ms

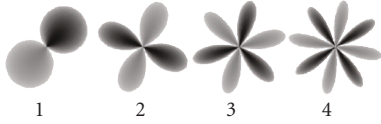


FIGURE 14: Rotated elementary directivity functions.

type of sources made in Section 2.3. However, *AvCo* and particularly *Meq* methods enables to limit the standard deviation of  $MAG_{\Psi_m}$  to similar values than other sources (see Figures 12(a) and 13(a)).

The reproduction accuracy (standard deviation of  $MAG_{\Psi_m}$ ) is best for omnidirectional sources and degrades with the absolute value of the source degree (see Figures 12(b) and 13(b)). This means that the more complex the directivity characteristics are, the lower is the accuracy.

The accuracy is independent of listening distance (see Figures 12(c) and 13(c)). This is the case even for the *Meq* method even if filters are calculated to minimize the reproduction error for  $\gamma = -2$  m only.

For  $GD_{\Psi_m}$ , the mean value and the standard deviation are only given for each equalization method considering all measuring positions, all source positions, and all source degrees. They are shown for both ideal and MAP loudspeakers in Table 1. Only small differences are observed between the various equalization methods. Only for MAP loudspeakers, the *Meq* method performs slightly better but does not compensate for all reproduction artifacts.

As for  $MAG_{\Psi_m}$ , source position dependency, source degree dependency, and measuring distance dependency analysis were performed but are not shown here. They exhibit similar, but less pronounced, tendencies concerning temporal reproduction accuracy than for  $MAG_{\Psi_m}$ . Accuracy is worst for close sources to the array and for high absolute source degrees. However, the standard deviation never exceeds 2 milliseconds which is below the audible threshold for coloration artifacts [28] even for sensible conditions (anechoic conditions, transient signal).

#### 4.3.2. Rotated elementary directivity functions

In this section, the directivity characteristics under study may be expressed as  $\cos(m(\phi - \pi/4m))$ . They are obtained by rotating the elementary directivity function of degree  $m$  at an intermediate position between degree  $-m$  and degree  $m$  (see Figures 2 and 14). In the following, they are referred to as rotated elementary directivity functions of degree  $m$ .

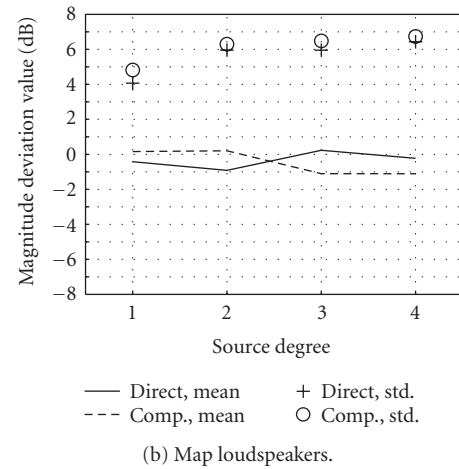
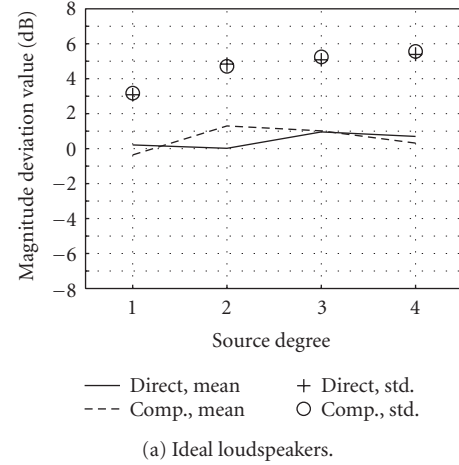


FIGURE 15: Mean value and standard deviation of  $MAG_{\Psi_m}$  evaluated below the aliasing frequency for all microphone and source positions. Synthesis of rotated elementary directivity function (see (22)). Comparison between recomposition from elementary directivity (comp) and direct synthesis (direct). All filters are calculated using individual equalization + average synthesis error compensation (*AvCo*).

Trigonometrical identities enable to express them as a combination of elementary directivity functions of degree  $-m$  and  $m$ :

$$\cos\left(m\left(\phi - \frac{\pi}{4m}\right)\right) = \frac{1}{\sqrt{2}}(\cos(m\phi) + \sin(m\phi)). \quad (22)$$

These characteristics can thus be synthesized using whether a direct synthesis specifying the required radiation characteristics as the target sound field, either by combining filters obtained for the same source position for degree  $-m$  and  $m$ .

Figures 15 and 16 show mean values and standard deviation of  $MAG_{\Psi_m}$  comparing direct synthesis (direct) and composition (comp) of filters calculated for degree  $-m$  and  $m$ . Results are given for each degree of rotated elementary directivity function for both ideal loudspeakers (Figures 15(a) and 16(a)) and MAP loudspeakers (Figures 15(b) and 16(b) and

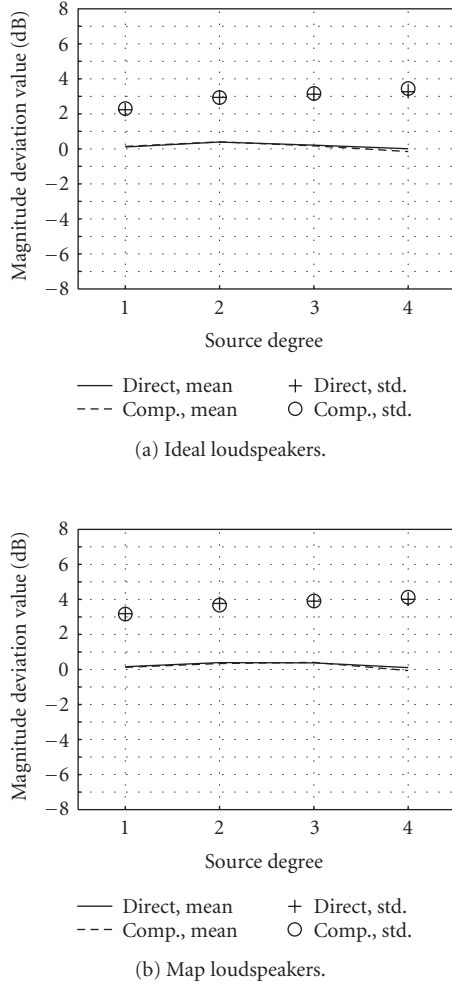


FIGURE 16: Mean value and standard deviation of  $MAG_{\Psi_m}$  evaluated below the aliasing frequency for all microphone and source positions. Synthesis of rotated elementary directivity function (see (22)). Comparison between recomposition from elementary directivity (comp) and direct synthesis (direct). All filters are calculated using multichannel equalization (Meq).

16(b)) considering all source and microphone positions. In Figure 15, all filters are calculated using the *AvCo* method. Figure 16 displays results for filters calculated using the *Meq* method. For both equalization methods, “direct” or “comp” synthesis of rotated elementary directivity functions exhibit similar tendencies with respect to degree  $m$ . As in the case of elementary directivity functions, the accuracy generally degrades with increasing degrees.

The *Meq* method performs better than the *AvCo* method. Using the *Meq* method, the “direct” or the “comp” synthesis perform very similar. The difference between mean values or between standard deviations is less than 0.2 dB for all situations (see Figure 16). For the *AvCo* method, this difference can be as large as 1.5 dB (mean values of  $MAG_{\Psi_m}$  for degree 2, see Figure 15(a)). This mean value deviation may be problematic while combining these rotated elementary directivity

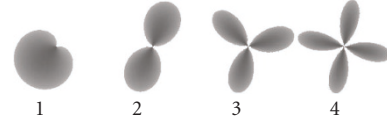


FIGURE 17: “Combined” directivities.

functions with another elementary directivity function as proposed in the next section.

#### 4.3.3. Combined directivities

The reproduction accuracy is estimated for another type of composite directivity, referred to as “combined” directivity, which is defined as a combination of rotated elementary directivity functions and the elementary directivity function of degree 0 (omni):

$$\Phi_m(\phi) = \frac{0.5}{\sqrt{2}} (\cos(m\phi) + \sin(m\phi)) + 0.5. \quad (23)$$

The characteristics of the “combined” directivities of degrees 1 to 4 are displayed in Figure 17. Considering visibility criteria of the test source positions (cf. Figure 11), only the lower quarter or the lower half of the directivity figure is synthesized within the listening area. Therefore, the synthesized directivity figure is a beam which becomes sharper with increasing degree.

The test situations are the same as for rotated elementary directivity functions. Accuracy results are displayed in Figures 18 and 19. The synthesized sound field for the reproduction of these “combined” directivities exhibits large inaccuracies when using the *AvCo* method. The errors are particularly large for direct synthesis of “combined” directivities of degrees 3 and 4. The standard deviation of  $MAG_{\Psi_m}$  is even out of bounds ( $> 8$  dB) considering both ideal and MAP loudspeakers for sources of degree 4. The “comp” synthesis exhibits lower standard deviation of  $MAG_{\Psi_m}$  but high mean values ( $\approx 6$  dB). The *Meq* method limits the reproduction error. The difference between direct and composition is below 0.5 dB considering mean values of  $MAG_{\Psi_m}$ . This difference increases to 1 dB for the standard deviation of  $MAG_{\Psi_m}$ .

#### 4.4. Discussion and real-time rendering

In this section, three different equalization methods were used in order to compensate for rendering deficiencies while synthesizing directional virtual sources using WFS. It could be seen that the more complex techniques (*Meq* and *AvCo*) are also the more efficient ones and that efficiency increases with complexity.

The equalization process can be regarded as an advanced calibration procedure that has to be done once for a given system. The *Meq* and *AvCo* methods require to estimate (and invert) the free field loudspeaker response at an ensemble of listening position for each and every source position and directivity function. This can appear as a cumbersome task.

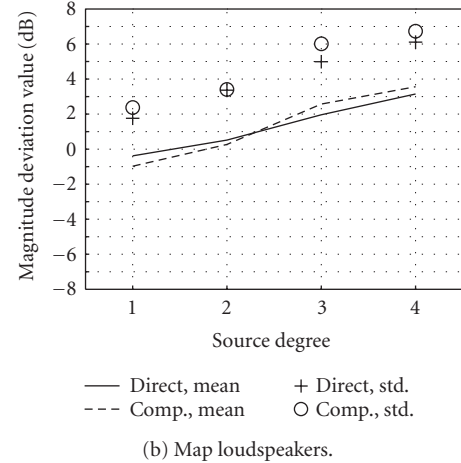
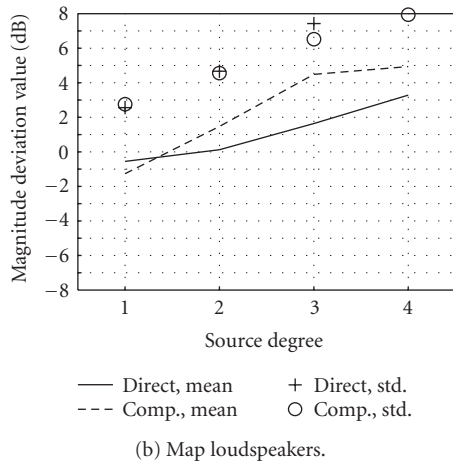
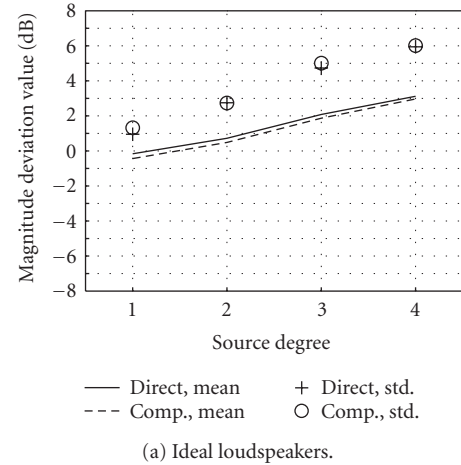
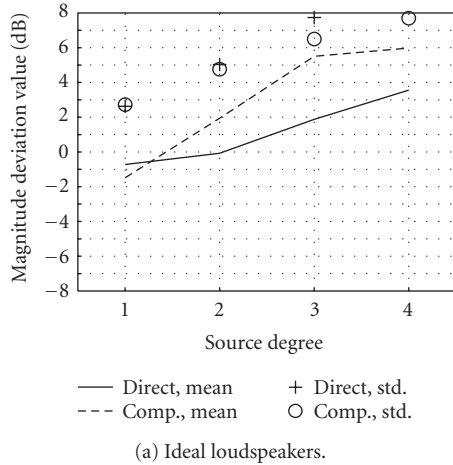


FIGURE 18: Mean value and standard deviation of  $MAG_{\psi_m}$  evaluated below the aliasing frequency for all microphone and source positions. Synthesis of “combined” directivity (cf. (23)). Comparison between recomposition from elementary directivity (comp) and direct synthesis (direct). All filters are calculated using individual equalization + average synthesis error compensation (AvCo).

FIGURE 19: Mean value and standard deviation of  $MAG_{\psi_m}$  evaluated below the aliasing frequency for all microphone and source positions. Synthesis of “combined” directivity (cf. (23)). Comparison between recomposition from elementary directivity (recomp) and direct synthesis (direct). All filters are calculated using multi-channel equalization (Meq).

However, one should take into account the limited localization resolution of the human auditory system [29] in order to define a finite size database of source positions for a given setup [11, 18]. For the system described in Section 4.1, about six hundred source positions should be considered. The spherical harmonic representation enables one to restrict the “infinite” directivity space to a finite number of elements. The current implementation considers elementary directivity functions of degree  $-2$  to  $2$ . Therefore, about three thousand filters should be calculated per loudspeaker and stored in a database. For the *Meq* method, this takes about fifty hours on a modern PC having two 2 GHz dual core processors on a not fully optimized code under Matlab™. The *AvCo* method is “only” five to six times more efficient since for all sources the loudspeaker array response has to be computed and smoothed on numerous microphone positions. The *Ind* method has much lower complexity since only one

filter per loudspeaker has to be computed for all sources. It is also, by far, the least effective.

The three methods provide filters of same sizes (800 taps at 48 kHz in the current implementation) together with an ensemble of delays for each loudspeaker and each considered virtual source. Therefore, the real-time processing load is the same for both the *Meq* and *AvCo* methods. It is only lower for the *Ind* since the filters do not depend on the virtual source characteristics.

Figure 20 presents the architecture of a typical WFS rendering system. The complete system has a network structure. Rendering modules are associated with a group of loudspeakers. They get audio streams and “scene description parameters” as an input from a communication network [30]. The scene-description parameters contain data describing, for each source, its position and directivity characteristics. Each of the rendering modules has its own database of

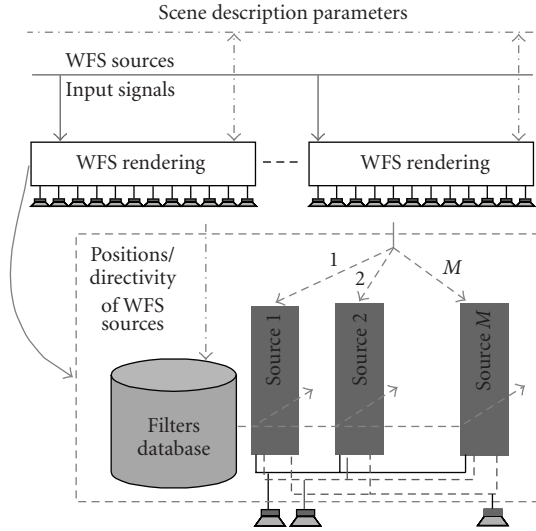


FIGURE 20: WFS system rendering architecture.

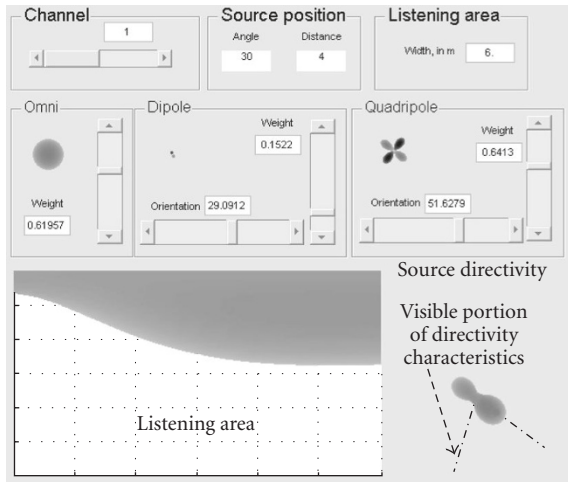


FIGURE 21: M3S directivity interface.

pre-calculated filters for the ensemble of loudspeakers it is attached to. The current implementation of WFS rendering supports real-time synthesis and manipulation of directional sources as a weighted sum of elementary directivity functions from degree  $-2$  to degree  $2$ . For a more intuitive manipulation, elementary directivity functions are grouped by same “absolute degree” ( $0$ : omni,  $-1/1$ : dipole,  $-2/2$ : quadripole). For each absolute degree, a level and an orientation parameter are defined. They enable one to synthesize both elementary directivity functions and directivity combinations using basic trigonometrical identities.

A directivity manipulation and visualization interface is presented in Figure 21. For each virtual source, source position and directivity parameters are manipulated and transmitted to the communication network [30]. A visual

representation of the synthesized directivity is displayed for each absolute degree next to the manipulated parameters. The interface also displays the composite directivity together with the visibility angle of the source through the loudspeaker array. The latter describes the visible portion of the directivity characteristics within the listening area. This is further displayed on a global view which represents the attenuation factor due to the synthesized directivity depending on the listening position.

The proposed interface remains limited to the visualization of directivity for a unique source. More advanced interfaces may be used combining a visualization of the spatial organization of the sound scene (position of sources) together with directivity information. For example, a representation of the source directivity may be displayed in the background of the interface as proposed by Delerue [31].

## 5. APPLICATIONS OF DIRECTIONAL SOURCES FOR WAVE FIELD SYNTHESIS

In this section, applications of directional sources for WFS are discussed. They concern direct sound manipulation and interaction with the listening environment.

### 5.1. Direct sound manipulation

As a holophonic sound reproduction technique, WFS targets the synthesis of the physical characteristics of sound fields within an extended listening area. Contrary to sweet-spot-based techniques (stereo, 5.1, first-order ambisonics), the listener may experience natural variations in perception of the various sound sources while wander in the WFS installation. The localization may vary according to the relative position of listener and the sound sources (parallax effect) independently of the loudspeakers’ position [32]. Natural modification of level or sound color can be perceived. The virtual environment therefore provides coherent proprioceptive and auditory cues to the listener which increase the sensation of presence [33].

Directivity can be used as a tool to create or increase disparities within the listening area. Sound sources are given a directional radiation pattern such that they are heard preferably in a portion of the listening area. In the context of sound installations [34], “unnatural” sound sources may be created. For example, a “two-mouth head” may be synthesized using a source of degree  $-2$  which creates a zero in front and lobes to the sides. More realistic approaches could be envisaged such as an attempt of “spatial additive synthesis” [35] where the output of the different vibration modes of an instrument to be reproduced or synthesized would be coupled with corresponding directional sources. An approach to record and reproduce sound source directivity has also been presented by Jacques et al. [36]. It is based on multimicrophone recordings that are mapped to directional sources reproduced on a WFS setup.

These approaches are bound to the limitations of the synthesis of directional sources using WFS (horizontal directivity dependency only, reduced visibility, below the

aliasing frequency). However, informal listening sessions could demonstrate the benefit of the reproduction of directive sources. More studies are required to evaluate the perceptual effect of these inaccuracies.

### 5.2. Interaction with listening environment

Recent studies have described the interaction of a linear WFS array with the listening environment [11, 37–39]. Below the aliasing frequency, the loudspeaker array may be regarded as an aperture through which the sound field of the target source propagates. Considering the horizontal plane, the loudspeaker array radiates sound energy mostly within the visibility area of the source through the loudspeaker array [11, 38]. Outside of the horizontal plane, the emitted sound field manifests a symmetry around the axis of the loudspeaker array.

The total acoustic power emitted by the array is dependent both on source position and source directivity, more exactly on the portion of the source directivity which is visible through the loudspeaker array [38]. The level of the reverberant field is proportional to the total acoustic power emitted by the array. Therefore, directivity may be used to partly control the level of natural reverberated field within the environment.

In [39], Caulkins et al. describe measurements of a WFS array in a concert hall using a high spatial resolution microphone [40]. These measurements provide a spatiotemporal description of the early room effect. It is shown that directional sources can be used to create lateral reflections while eliminating the direct sound at the position of the microphone. This is achieved by synthesizing sources that present a zero at listening positions and have lobes that illuminate side walls. Alternatively, a directivity beam can be created in order to emit sound energy preferably in the direction of the listening area while limiting the energy radiated to the sides [39]. Directivity can thus be used to manipulate the early room effect which is related to perceptual attributes such as apparent source width or room envelopment.

A similar effect can be obtained using a 3D array of loudspeakers (“la Timée”) and is described in [41]. This device enables the synthesis of directivity over the entire solid angle as a combination of a monopole and 3 orthogonal dipoles. Unlike WFS, directional sources can only be synthesized at the position of this directivity controllable loudspeaker.

## 6. CONCLUSION

The synthesis of directional sound sources using WFS was presented in this article. The proposed formulation relies on the synthesis of elementary directivity functions based on a subset of spherical harmonics. This versatile representation allows for manipulations of directivity characteristics as a weighted sum of elementary directivity functions.

Limitations are however to be expected while synthesizing directive characteristics for virtual sources. Only horizontal dependencies in directivity characteristics can be

reproduced. Because of the finite length of the loudspeaker array, synthesis is only possible within a visibility window. The finite number of loudspeakers also restricts the proper reconstruction of wave fronts below the so-called aliasing frequency. Apart from these spatial and frequency related limitations, the limited validity of the proposed approximations to derive WFS introduces artifacts even when ideal omnidirectional loudspeakers are used.

Equalization techniques should be used to reduce these artifacts and to compensate for the radiation characteristics of real loudspeakers. An extensive study on reproduction accuracy of elementary directivity functions and composite directivity figures was performed to compare the performance of three equalization techniques for both ideal and real loudspeakers. It was shown that the proposed multichannel equalization technique enables to reduce reproduction artifacts within an extended listening area. Moreover, this method ensures that composite directivities are properly synthesized as a weighted sum of elementary directivity functions. It thus allows real-time manipulations of directivity characteristics with limited reconstruction errors below the spatial aliasing frequency.

Applications of directional sources for WFS were finally discussed in the context of virtual or augmented environments. Directivity allows one to model and reproduce natural or unnatural disparities of the sound scene within an extended listening area. It also provides control parameters for adjusting the interaction of the loudspeaker array with the listening environment (early room effect, level of reverberant field).

## ACKNOWLEDGMENTS

The author would like to thank Olivier Warusfel and Terence Caulkins for fruitful comments and discussions on the topic. Thanks a lot to the anonymous reviewers for helpful comments on the initial manuscript.

## REFERENCES

- [1] A. J. Berkhou, D. de Vries, and P. Vogel, “Acoustic control by wave field synthesis,” *Journal of the Acoustical Society of America*, vol. 93, no. 5, pp. 2764–2778, 1993.
- [2] E. W. Start, *Direct sound enhancement by wave field synthesis*, Ph.D. thesis, Delft University of Technology, Delft, Pays Bas, The Netherlands, 1997.
- [3] R. Nicol, *Restitution sonore spatialisée sur une zone étendue: application à la téléprésence*, Ph.D. thesis, Université du Maine, Le Mans, France, 1999, [http://gyronymo.free.fr/audio3D/Guests/RozennNicol\\_PhD.html](http://gyronymo.free.fr/audio3D/Guests/RozennNicol_PhD.html).
- [4] O. Warusfel, E. Corteel, N. Misdariis, and T. Caulkins, “Reproduction of sound source directivity for future audio applications,” in *Proceedings of the 18th International Congress on Acoustics (ICA '04)*, Kyoto, Japan, April 2004.
- [5] S. Spors, A. Kuntz, and R. Rabenstein, “An approach to listening room compensation with wave field synthesis,” in *Proceedings of the 24th Convention of the Audio Engineering Society (AES '03)*, pp. 70–82, Banff, Canada, June 2003.

- [6] P.-A. Gauthier and A. Berry, "Adaptive wave field synthesis with independent radiation mode control for active sound field reproduction: theory," *Journal of the Acoustical Society of America*, vol. 119, no. 5, pp. 2721–2737, 2006.
- [7] E. N. G. Verheijen, *Sound reproduction by wave field synthesis*, Ph.D. thesis, Delft University of Technology, Delft, Pays Bas, The Netherlands, 1997.
- [8] E. G. Williams, *Fourier Acoustics: Sound Radiation and Nearfield Acoustical Holography*, Academic Press, San Diego, Calif, USA, 1999.
- [9] A. J. Berkhout, *Applied Seismic Wave Theory*, Elsevier, Amsterdam, The Netherlands, 1987.
- [10] M. Abramovitz and I. A. Stegun, *Handbook of Mathematical Functions*, Dover, New York, NY, USA, 9th edition, 1970.
- [11] E. Corteel, *Caractérisation et Extensions de la Wave Field Synthesis en conditions réelles d'écoute*, Ph.D. thesis, Université de Paris VI, Paris, France, 2004, <http://mediatheque.ircam.fr/articles/textes/Corteel04a/>.
- [12] E. Corteel, "On the use of irregularly spaced loudspeaker arrays for wave field synthesis, potential impact on spatial aliasing frequency," in *Proceedings of the 9th International Conference on Digital Audio Effects (DAFx '06)*, pp. 209–214, Montreal, Quebec, Canada, September 2006.
- [13] E. Corteel and R. Nicol, "Listening room compensation for wave field synthesis. What can be done?" in *Proceedings of the 23th Convention of the Audio Engineering Society (AES '03)*, Helsingør, Denmark, June 2003.
- [14] S. Spors, H. Buchner, and R. Rabenstein, "Adaptive listening room compensation for spatial audio systems," in *Proceedings of the 12th European Signal Processing Conference (EUSIPCO '04)*, Vienna, Austria, September 2004.
- [15] J. J. López, A. González, and L. Fuster, "Room compensation in wave field synthesis by means of multichannel inversion," in *Proceedings of IEEE Workshop on Applications of Signal Processing to Audio and Acoustics (WASPAA '05)*, pp. 146–149, New Paltz, NY, USA, October 2005.
- [16] E. Corteel, U. Horbach, and R. S. Pellegrini, "Multichannel inverse filtering of multiexciter distributed mode loudspeaker for wave field synthesis," in *Proceedings of the 112th Convention of the Audio Engineering Society (AES '02)*, Munich, Allemagne, Germany, May 2002.
- [17] P. A. Nelson, F. Orduña-Bustamante, and H. Hamada, "Multichannel signal processing techniques in the reproduction of sound," *Journal of the Audio Engineering Society*, vol. 44, no. 11, pp. 973–989, 1996.
- [18] E. Corteel, "Equalization in extended area using multichannel inversion and wave field synthesis," *Journal of the Audio Engineering Society*, vol. 54, no. 12, 2006.
- [19] R. van Zon, E. Corteel, D. de Vries, and O. Warusfel, "Multi-actuator panel (map) loudspeakers: how to compensate for their mutual reflections?" in *Proceedings of the 116th Convention of the Audio Engineering Society (AES '04)*, Berlin, Allemagne, Germany, March 2004.
- [20] S. Spors, M. Renk, and R. Rabenstein, "Limiting effects of active room compensation using wave field synthesis," in *Proceedings of the 118th Convention of the Audio Engineering Society (AES '05)*, Barcelona, Spain, May 2005.
- [21] O. Kirkeby, P. A. Nelson, H. Hamada, and F. Orduña-Bustamante, "Fast deconvolution of multichannel systems using regularization," *IEEE Transactions on Speech and Audio Processing*, vol. 6, no. 2, pp. 189–194, 1998.
- [22] M. Guillaume, Y. Grenier, and G. Richard, "Iterative algorithms for multichannel equalization in sound reproduction systems," in *Proceedings of IEEE International Conference on Acoustics, Speech and Signal Processing (ICASSP '05)*, vol. 3, pp. 269–272, Philadelphia, Pa, USA, March 2005.
- [23] S. G. Norcross, G. A. Soulodre, and M. C. Lavoie, "Subjective investigations of inverse filtering," *Journal of the Audio Engineering Society*, vol. 52, no. 10, pp. 1003–1028, 2004.
- [24] M. Bouchard, "Multichannel affine and fast affine projection algorithms for active noise control and acoustic equalization systems," *IEEE Transactions on Speech and Audio Processing*, vol. 11, no. 1, pp. 54–60, 2003.
- [25] M. M. Boone and W. P. J. de Bruijn, "On the applicability of distributed mode loudspeakers panels for wave field synthesis sound reproduction," in *Proceedings of the 108th Convention of the Audio Engineering Society (AES '00)*, Paris, France, February 2000.
- [26] M. M. Boone, "Multi-actuator panels (maps) as loudspeaker arrays for wave field synthesis," *Journal of the Audio Engineering Society*, vol. 52, no. 7-8, pp. 712–723, 2004.
- [27] M. Slaney, "An efficient implementation of the patterson-holdsworth filter bank," Tech. Rep. 35, Apple Computer, Cupertino, Calif, USA, 1993.
- [28] S. Flanagan, B. C. J. Moore, and M. A. Stone, "Discrimination of group delay in clicklike signals presented via headphones and loudspeakers," *Journal of the Audio Engineering Society*, vol. 53, no. 7-8, pp. 593–611, 2005.
- [29] J. Blauert, *Spatial Hearing, The Psychophysics of Human Sound Localization*, MIT Press, Cambridge, Mass, USA, 1999.
- [30] R. Pellegrini, M. Rosenthal, and C. Kuhn, "Wave field synthesis: open system architecture using distributed processing," in *Forum Acusticum*, Budapest, Hungary, September 2005.
- [31] O. Delerue, "Visualization of perceptual parameters in interactive user interfaces: application to the control of sound spatialization," in *Proceedings of the 120th Convention of Audio Engineering Society (AES '06)*, Paris, France, May 2006.
- [32] M. Noguès, E. Corteel, and O. Warusfel, "Monitoring distance effect with wave field synthesis," in *Proceedings of the 6th International Conference on Digital Audio Effects (DAFx '03)*, London, UK, September 2003.
- [33] O. Warusfel and I. Viaud-Delmon, "Contribution of interactive 3D sound to presence," in *Proceedings of the 6th International Workshop on Presence*, Aalborg, Denmark, October 2003.
- [34] G. Grand, E. Corteel, and R. Kronenber, "L'amiral cherche une maison à louer," Sound installation, Centre Georges Pompidou, DADA exhibition, October 2005–January 2006, 2005.
- [35] O. Warusfel, N. Misdariis, T. Caulkins, and E. Corteel, "Radiation control applied to sound synthesis: an attempt for "spatial additive synthesis"" in *Proceedings of the 147th Meeting of the Acoustical Society of America (ASA '04)*, New York, NY, USA, May 2004.
- [36] R. Jacques, B. Albrecht, F. Melchior, and D. de Vries, "An approach for multichannel recording and reproduction of sound source directivity," in *Proceedings of the 119th Convention of the Audio Engineering Society (AES '05)*, New York, NY, USA, October 2005.
- [37] T. Caulkins, E. Corteel, and O. Warusfel, "Wave field synthesis interaction with the listening environment, improvements in the reproduction of virtual sources located inside the listening room," in *Proceedings of the 6th International Conference on Digital Audio Effects (DAFx '03)*, London, UK, September 2003.
- [38] T. Caulkins and O. Warusfel, "Characterization of the reverberant sound field emitted by a wave field synthesis driven loudspeaker array," in *Proceedings of the 120th Convention of*

*the Audio Engineering Society (AES '06)*, Paris, France, May 2006.

- [39] T. Caulkins, A. Laborie, E. Corteel, R. Bruno, S. Montoya, and O. Warusfel, "Use of a high spatial resolution microphone to characterize the early reflections generated by a WFS loudspeaker array," in *Proceedings of the 28th Convention of the Audio Engineering Society (AES '06)*, Pitea, Sweden, June 2006.
- [40] A. Laborie, R. Bruno, and S. Montoya, "A new comprehensive approach of surround sound recording," in *Proceedings of the 114th Convention of the Audio Engineering Society (AES '03)*, Amsterdam, Pays Bas, The Netherlands, March 2003.
- [41] O. Warusfel and N. Misdariis, "Directivity synthesis with a 3D array of loudspeakers, application for stage performance," in *Proceedings of the International Conference on Digital Audio Effects (DAFx '01)*, Limerick, Ireland, December 2001.

---

**E. Corteel** was born in Vernon, France, in 1978. He received an M.Sc. degree in telecommunication engineering in 2000 and a Ph.D. degree in acoustics and signal processing from Paris 6 University, Paris, France, in 2004. He joined Studer Professional Audio AG in 2001 where he started to work on wave field synthesis in the context of the European Carrouso IST project no. 1999-20993. He followed up this research at



IRCAM, Paris, France, between 2002 and 2004. Since 2005, he has shared his time between IRCAM and Sonic Emotion, Oberglatt, Switzerland. His research interests include the design and evaluation of spatial sound rendering techniques for virtual or augmented reality applications (sound installations, concerts, simulation environments, etc.), as well as spatial hearing and crossmodal interactions.